Indirect Rotor Field Orientation Vector Control for Induction Motor Drives in the Absence of Current Sensors

Z. S. WANG[*], S. L. HO[**]
[*] College of Electrical Engineering, Zhejiang University, Hangzhou 310027, China
[**] Electrical Engineering Department of Hong Kong Polytechnic University, Hong Kong
zjuwzs@hotmail.com, eeslho@inet.polyu.edu.hk

***Abstract*—This paper proposes a simplified vector control implementation strategy that can be realized in the absence of current sensors. In order to decouple the torque and flux in the determination of the three-phase voltage reference commands of the SPWM inverter, both stator and rotor currents in the stationary and rotating frames can be derived from the corresponding rotor flux-oriented vector control requirements and motor dynamic equations. A sensitivity analysis to study the effect of parameter deviation or mismatch is also investigated. Simulation results are presented to demonstrate the feasibility and performance of the proposed methodology.**

Keywords- vector control; induction motor control; motor drives

I. INTRODUCTION

The indirect field orientation control (IFOC) strategy is widely used for implementing high performance induction motor drive systems, and has been increasingly adopted as the standard industry solution [1-3]. In this scheme, current sensors are used to measure the motor currents, and two current controllers have to be designed to regulate the motor currents and to infer the M/T-axis voltage reference command. These sensors and controllers not only increase the overall system's cost, but also increase the design complexity in terms of drift compensation and gain correction, particularly if the scheme is to be applicable over the whole speed and torque load ranges.

Conventional slip frequency control scheme does not use voltage and current sensors [4]. However, essentially, it is scalar control. Inevitably, its dynamic performance is poor due to the coupling effect between torque and flux. Yamamura S. etc. integrated the scalar scheme with vector control, and proposed the slip frequency vector control strategy to get good dynamic responds [5]. But in this method, current sensors and their corresponding controllers have to be designed to regulate the motor currents.

This paper presents a novel IFOC implementation method for induction motor drives without the need to use voltage and current sensors. It also eliminates two current feedback loops and their associated controllers, resulting in overall design simplicity and cost reduction for vector controllers. In order to realize the decoupled control between the torque and flux, the stator current is separated into two orthogonal components for torque current and flux magnetizing current, and these components are then regulated independently. Furthermore, it can be shown that if the rotor currents are known values, the voltage applied to the motor can be determined using motor equations. Nevertheless the rotor current cannot be measured directly in induction motors. However, for rotor field orientation drives, one could calculate the rotor current based on the vector control scheme and motor dynamic equations. Thus, the voltage applied to the motor can be controlled precisely. On the other hand, one has to note that as there are no voltage and current feedbacks, the performance of the drive might deteriorate due to parameter deviations/mismatch and disturbances in the input DC link voltage. It is shown from the simulation results that even though there are large value mismatching in parameters, the proposed algorithm could, with the exception of very low speeds, produce good dynamic and steady state performances over a wide range of speed. The effect of DC link voltage disturbance can be neglected in many actual practical application cases.

II. INDUCTION MOTOR MODEL AND THE PROPOSED CONTROL METHODOLOGY

According to the rotor field orientation vector control theory [4] [6], the stator current of squirrel-cage induction motor can be decomposed into two orthogonal components in the synchronous rotating rotor flux-oriented reference frame (M-T frame) which are, namely, the torque current i_{TS} , which is to generate the electromagnetic torque, and the magnetizing current i_{MS} , which is to excite the motor flux. These two current components are separated independently and decoupled each other. Their magnitudes can be calculated according the electromagnetic torque (T_e) and rotor flux level (λ_r), and are governed by the following equations [6]

$$\begin{cases} i_{TS} = \dfrac{4T_e}{3P\lambda_r} \\ i_{MS} = \dfrac{1+(L_r/R_r)p}{L_M}\lambda_r \end{cases} \tag{1}$$

The subscript s and r indicate the stator and rotor variables, M,T represent the variables in the rotor field orientation rotating reference frame. R_r , L_M , L_S and L_r are the motor rotor resistance, mutual inductance, stator inductance and rotor inductance, respectively. λ_r and T_e are the respective rotor flux and electromagnetic torque. P is the number of pole pairs. p is the d/dt operator.

In most cases, the flux magnitude should be kept at some constant level, particularly when the motor runs below its base speed. So, (1) can be rewritten as

$$\begin{cases} i_{TS} = \dfrac{4T_e}{3P\lambda_r} \\ i_{MS} = \dfrac{\lambda_r}{L_M} \end{cases} \tag{2}$$

The current angle θ_2 in M-T axis is

$$\theta_2 = arctg\frac{i_{TS}}{i_{MS}} \tag{3}$$

On the other hand, the slip frequency is [4]

$$\omega_s = \frac{R_r i_{TS}}{L_r i_{MS}} \tag{4}$$

The rotor flux angle in stationary reference frame can be expressed as

$$\theta_1 = \int(\omega_r + \omega_s)dt \tag{5}$$

where ω_r is the rotor mechanical speed. Thus, the stator current can be expressed in the stationary reference frame as:

$$\begin{bmatrix} i_{\alpha s} \\ i_{\beta s} \end{bmatrix} = \begin{bmatrix} cos\theta_1 & -sin\theta_1 \\ sin\theta_1 & cos\theta_1 \end{bmatrix} \begin{bmatrix} i_{MS} \\ i_{TS} \end{bmatrix} \tag{6}$$

On the hand, in the rotor flux-orientated reference frame, the rotor side voltage-current equations of squirrel-cage induction motor can be described as [6]

$$\begin{bmatrix} 0 \\ 0 \end{bmatrix} = \begin{bmatrix} L_M p & 0 \\ L_M \omega_s & 0 \end{bmatrix} \begin{bmatrix} i_{MS} \\ i_{TS} \end{bmatrix} + \begin{bmatrix} R_r + L_r p & 0 \\ L_r \omega_S & R_r \end{bmatrix} \begin{bmatrix} i_{Mr} \\ i_{Tr} \end{bmatrix} \tag{7}$$

where i_{Mr}, i_{Tr} are rotor current components in M-T axis.

The first row of (7) can be rewritten as

$$\begin{aligned} 0 &= R_r i_{Mr} + p(L_M i_{Ms} + L_r i_{Mr}) \\ &= R_r i_{Mr} + p\lambda_{Mr} \end{aligned} \tag{8}$$

In the rotor field orientation control, $\lambda_r = \lambda_{Mr}, \lambda_{Tr} = 0$. In most cases, flux magnitude should be kept at some constant levels: $|\lambda_r| = const.$, or $p\lambda_r = 0$. Base on these requirements and the flux definition, the rotor current components in M-T axis, i_{Mr}, i_{Tr}, can be obtained as [6]

$$\begin{cases} i_{Mr} = -p\lambda_{Mr}/R_r = -p\lambda_r/R_r = 0 \\ i_{Tr} = (\lambda_{Tr} - L_m i_{Ts})/L_r = (0 - \mathrm{L}_M/\mathrm{L}_r)\, i_{Ts} \\ \quad = -(\mathrm{L}_M/\mathrm{L}_r)\, i_{Ts} \end{cases} \tag{9}$$

Using coordinate transformation, the rotor current can be expressed in the stationary reference as

$$\begin{bmatrix} i_{\alpha r} \\ i_{\beta r} \end{bmatrix} = \begin{bmatrix} cos\theta_1 & -sin\theta_1 \\ sin\theta_1 & cos\theta_1 \end{bmatrix} \begin{bmatrix} i_{Mr} \\ i_{Tr} \end{bmatrix} \tag{10}$$

The phasor diagram of the stator and rotor current (i_s, i_r) in $\alpha-\beta$ axis and M-T axis is shown in Fig. 1.

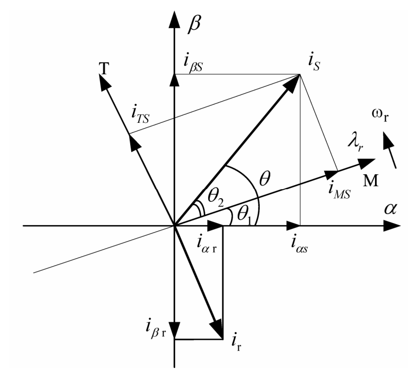

Fig.1 Phasor diagram of stator and rotor current

Based on the motor voltage-current equations in stationary reference frame which are shown below,

$$\begin{bmatrix} u_{\alpha s} \\ u_{\beta s} \end{bmatrix} = \begin{bmatrix} R_S + L_S p & 0 \\ 0 & R_S + L_S p \end{bmatrix} \begin{bmatrix} i_{\alpha s} \\ i_{\beta s} \end{bmatrix} + \begin{bmatrix} L_M p & 0 \\ 0 & L_M p \end{bmatrix} \begin{bmatrix} i_{\alpha r} \\ i_{\beta r} \end{bmatrix} \tag{11}$$

where R_s, L_s are stator resistance and inductance. Using the 2-phase to 3-phase coordinate transformation, the three phase reference command voltage signal can finally be determined.

Thus, the final stator voltage, including frequency, phase and magnitude, can be directly derived from the motor dynamic equations just according to the speed and flux requirements (reference). Any voltage current sensors, signal feedback loops, and corresponding controllers do not need. Moreover, this method does not require complicated algorithm [5][6], and time-consuming parameter online identification technique [6]. So, the proposed control scheme can greatly simplify the system design, and reduce overall cost.

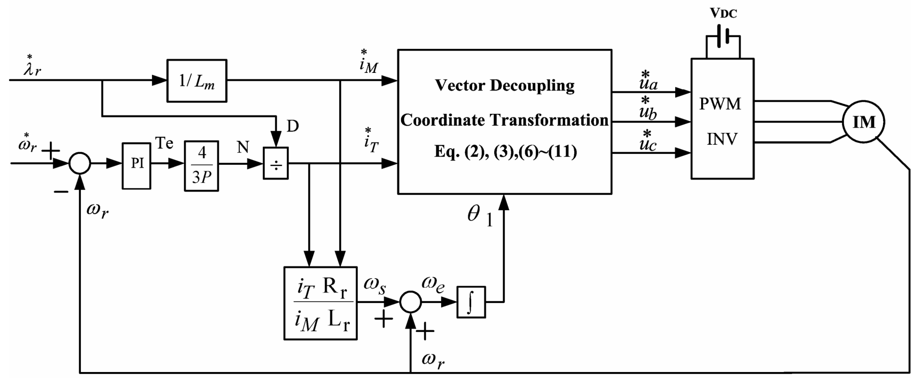

Fig.2 Configuration o the proposed vector control method

III. Simulation Results

Digital simulation research is carried out to validate the proposed control method. Fig. 2 shows the system configuration of the vector control: a 2.2 kW induction motor is driven by a SPWM voltage-type inverter, and the three-phase voltage reference command applied to the inverter is derived from the flux and torque references. The simulation investigation is focused on the motor performance with decoupled torque and flux, a sensitivity study to evaluate parameter mismatch or deviation, and the tracking ability of the motor in detuned cases. The motor parameters are $R_S = 3\,\Omega$, $R_r = 3.23\,\Omega$, $L_M = 210mH$, $L_S = L_r = 223mH$, *P*=2.

A. Performance of the Proposed IFO Conreoller

Detailed simulation tests are carried out to assess the proposed control method.

Figs. 3 and 4 show the torque and flux decoupled performance of the motor. In Fig. 3, the motor is running at a speed of 1000 rpm. It can be seen that as the load torque is suddenly changed from 5.5 Nm to 10.5 Nm (trace a), the rotor flux level hardly changes (trace b, c), although there is a small speed dip but then it is restored quickly (trace d). Fig. 4 shows a different case in that the flux level is suddenly changed at t=5 s by the manipulators (trace a, c), however the torque can be restored to its original level quickly (trace b). Fig. 5 shows the tracking performance of the motor following a trapezoidal speed reference (trace a). Trace b is the speed error, and trace c is the rotor flux in the $\alpha - axis$. It can be seen that the flux level can be kept constant in different speed regions. The M-axis and the T-axis fluxes in trace d illustrate the effect of the rotor field-oriented control: $\lambda_{T\,r} = 0$, $\lambda_{M\,r} = const.$ The speed tracking experiment is in a constant load condition (10Nm). This trapezoidal test can be used to evaluate the driver running in bi-direction operation, constant /variable speed and motoring/generative modes.

Fig. 6 shows the speed transient and step torque change responses (trace a). The load torque is proportional to the rotor speed in this case. There are speed reference and load torque step changes at time t=3 s and at t=3.5 s (trace a, c) respectively. Trace d and b show the corresponding flux magnitude and $\alpha -$ axis flux.

Because there are no voltage and current feedbacks in this control method, parameter mismatching or detuned running is a major problem. The following tests are designed to evaluate this performance. In Fig.7, the DC link voltage, which is applied to the inverter, is set to have a $\pm$ 20% deviation from the rated voltages (the rated voltage is 500V) (trace a). It shows that the steady state torque is not changed (trace c), but the flux level is changed by as much as about $\pm$ 20%. This is still an acceptable result because in practical applications, most motors have their own input voltage ranges and their corresponding flux levels. Moreover, many new generation drivers use power factor correction (PFC) circuits in the first stage, so that their DC link voltage can be maintained at a constant level, and therefore one does not need to take into account this influence.

Fig. 8 shows the flux sensitivity with respect to the inductor parameters (L_M, L_S, L_r) and mismatching in low-speed (100rpm, traces a, b) and high-speed (1200 rpm, trace c, d) running. During t=2s to 3s, $\hat{L}_{MSR} = L^*_{MSR}$. During t=3s to 4s, $\hat{L}_{MSR} = 2L^*_{MSR}$. During t=4s to 5s: $\hat{L}_{MSR} = 0.5L^*_{MSR}$, where L^*_{MSR} means the actual motor L_M , L_S , L_r parameters, and $\hat{L}_{MSR}$ means the corresponding mismatched parameters used in the controller. These mismatching has a slight influence upon the motor performance at high-speed running only, the influence is much more pronounced at low-speeds. The resistance mismatching influence is shown in Fig.9, similarly, it explains the flux level versus different stator and rotor resistances in low-speed (100rpm in trace a, b) and high-speed (1200 rpm in trace in trace d, e) regions. During t=2s to 3s, $\hat{R}_{s\,r} = R^*_{s\,r}$. During t=3s to 4s, $\hat{R}_{s\,r} = 2R^*_{s\,r}$. During t=4s to 5s, $\hat{R}_{s\,r} = 0.5R^*_{s\,r}$, where $R^*_{s\,r}$ means the actual parameters, and $\hat{R}_{s\,r}$ means the mismatched parameters used in the controller. One can

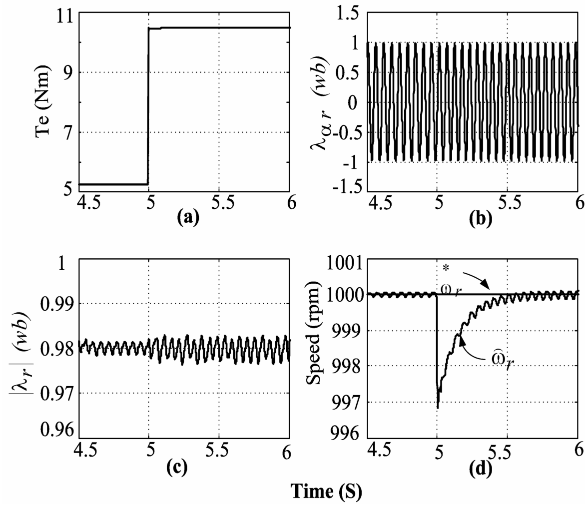

Fig.3 Flux performance under torque step changing

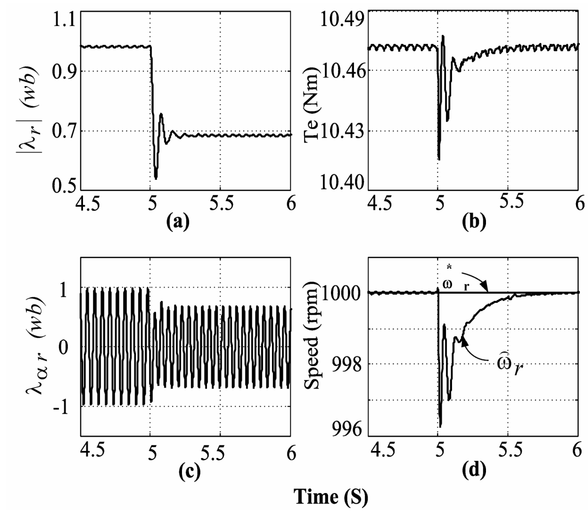

Fig.4 Torque performance under flux step changing

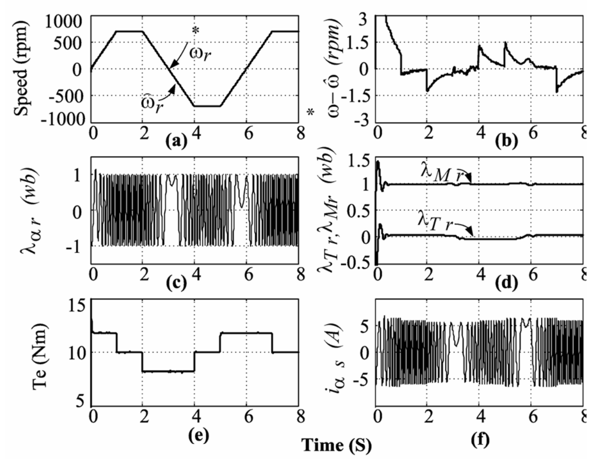

Fig.5 Trapezoidal tracking running

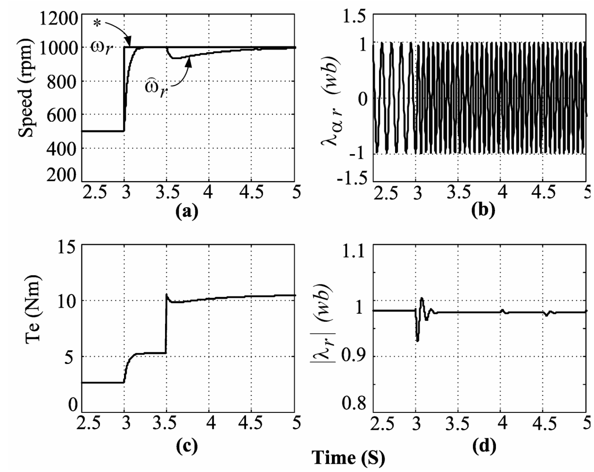

Fig. 6 Transient performance under step speed and load

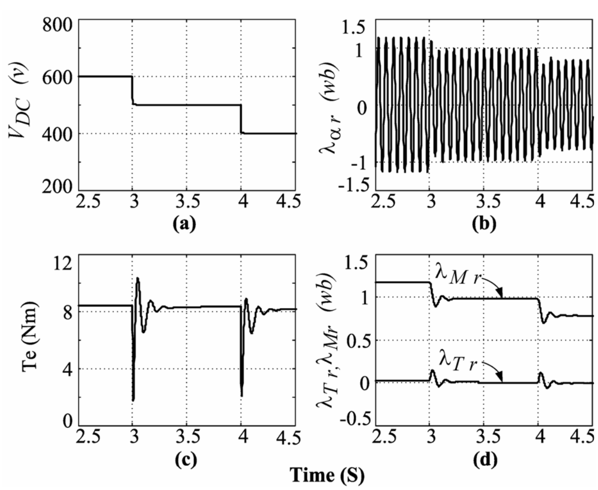

Fig. 7.Dc link voltage mismatching

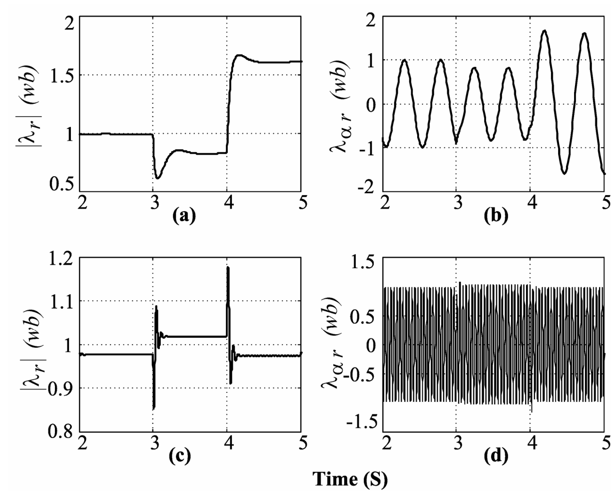

Fig.8 Inductor mismatching

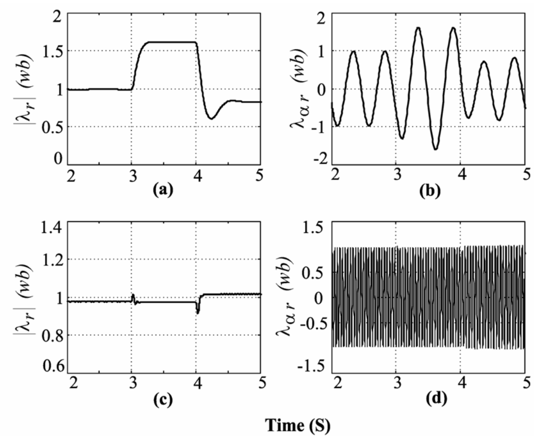

Fig.9 Resistance mismatching

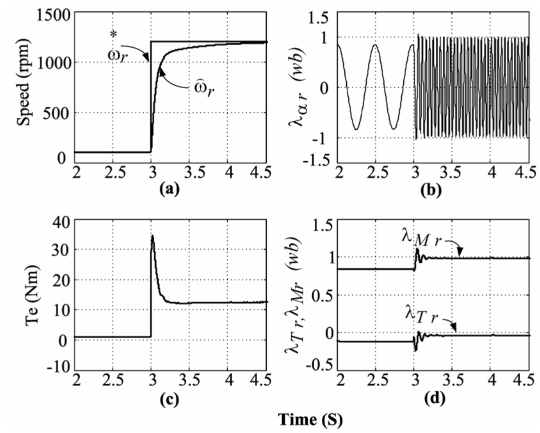

Fig. 10 Synthetic parameter mismatching

see that noticeable influence only appears in case of low speed running.

For the proposed control method, it will have a general tolerance to operate with parameters mismatching to a certain extent. A transient performance with parameter mismatching is shown in Fig. 10. The mismatched parameters are: $R^{*}{}_{s\,r} = 2\hat{R}_{s\,r}$, $L^{*}{}_{MSR} = 1.5\hat{L}_{MSR}$. The load is set to be proportional to the rotor speed. One can see that although the transient time is increased a bit, the steady state flux and torque (speed) are still stable with very small ripples.

B. Dynamic Responds Comparison with Conventional Vector Control

The proposed control algorithm is derived form the basic principle of rotor field orientation control. Consequently, so it is still vector control method. It should be noted that the purpose of this control method is aimed to reduce the money cost in hardware, and simplify the control design. Fig.11 shows the dynamic responds of conventional vector control and proposed control scheme in case of no load ((a)) and 10 Nm load (Trace (b)).

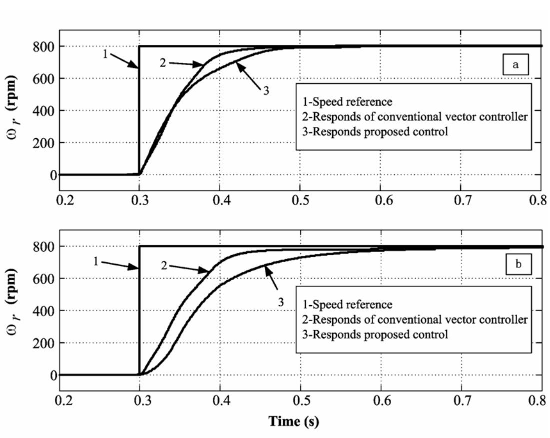

Fig. 11 Step responds of proposed control method and conventional vector control. (a). no load running, (b). running in 10 Nm load

Both trace (a) and (b) show that the proposed control scheme shares comparable good dynamic responds performance with conventional vector controller using current sensors no matter running in no load or in a heavy load.

IV. Conclusions

A vector control strategy for induction motor drives, which does not use current sensor, is proposed and tested. This scheme can reduce the system cost and simplify the control design. The current feedback loop and controller can be eliminated. It exhibits the decoupled effect between the flux and torque. Sensitivity to the parameter mismatching is evaluated by simulation, and it shows that the proposed algorithm works well over most speed ranges with the exception of low speeds. Moreover, the proposed system can operate stably with significant parameters mismatching as well.

References

[1] A. Consoli, G. Scarcella, and A. Testa, "Speed-and Current-Sensorless Field-Oriented Induction Motor Drive Operation at Low Stator Frequencies, " *IEEE Trans. Industry Applications*, Vol.40, No. 1, pp.186-193, Jan./Feb., 2004.

[2] Fang-Zheng Peng, and T. Fukao, Robust Speed Identification for Speed-sensorless Vector Control of Induction Motors, *IEEE Trans. Industry Appl.*, Vol.30, No. 5, pp.1234-1240, Sept./Oct., 1994.

[3] R. Gabriel, W. Leonard, C. Nordby, Field Oriented Control of a Standard AC Motor Using Micro-processors, *IEEE Trans. Industry Applications*, Vol.IA-16, No. 2, pp.186-192, 1980.

[4] Andrzej M. Trzynadlowski, *The Field Orientation Principle in Control of Induction Motors*, Kluwer Academic Publishers, U.S.A.

[5] Yamamura S., Spiral Vector Theory of AC Motor Analysis and Control, *IEEE Industry Applications Society Annual Meeting*, 1991, Conference Record of 1991, pp.79 – 86.

[6] Bose B. K., *Modern Power Electronics and AC Drivers*, Prentice-Hall, Englewood Cliffs, New Jersey, 1986.